

# Pulsed laser deposition of Cu:Al<sub>2</sub>O<sub>3</sub> nanocrystal thin films with high third-order optical susceptibility

J. M. Ballesteros,<sup>a)</sup> R. Serna, J. Solís, and C. N. Afonso  
*Instituto de Optica, C.S.I.C., Serrano 121, 28006 Madrid, Spain*

A. K. Petford-Long  
*Department of Materials, University of Oxford, Parks Road, Oxford OX1 3PH, United Kingdom*

D. H. Osborne and R. F. Haglund, Jr.  
*Department of Physics and Astronomy, Vanderbilt University, Nashville, Tennessee 37235*

(Received 14 April 1997; accepted for publication 27 August 1997)

Nanocomposite films comprising metal Cu nanocrystals embedded in an Al<sub>2</sub>O<sub>3</sub> matrix were deposited by alternating pulsed laser ablation from metallic Cu and ceramic Al<sub>2</sub>O<sub>3</sub> targets. The films were grown in vacuum on glass substrates held at room temperature. The as-grown films contain 4 nm Cu nanocrystals in an amorphous Al<sub>2</sub>O<sub>3</sub> matrix, with a total thickness of 190 nm. The films show a substantial third-order susceptibility with an electronic nonlinear refractive index of  $(2.93 \pm 1.08) \cdot 10^{-10} \text{ cm}^2 \text{ W}^{-1}$  and a nonlinear saturation of  $-(2.34 \pm 0.18) \cdot 10^{-5} \text{ cm W}^{-1}$ . © 1997 American Institute of Physics. [S0003-6951(97)03743-1]

Composite materials comprising metallic nanocrystals embedded in dielectric matrices exhibit interesting properties that can be engineered with the proper choice of metal and matrix. Such composites have been synthesized by quenching and heat treatments,<sup>1</sup> sol-gel processes,<sup>2</sup> sputtering co-deposition,<sup>3</sup> and ion implantation.<sup>4</sup> Most of these techniques are multi-step processes, in which a post-deposition treatment is often needed to optimize the properties. However, these treatments can also alter the average size, size distribution, and spatial arrangement of the nanoclusters,<sup>5,6</sup> with possible unfavorable effects particularly on the linear and nonlinear optical properties of the nanocomposite.

Unlike these methods, multiple-target sequential pulsed laser deposition (PLD), permits independent control of synthesis of the nanocrystals and the embedding matrix.<sup>7</sup> PLD has shown particular success in stoichiometric thin film deposition of complex oxides. Energetic (>100 eV) ions produced by ablation yield smooth, high-density films with good adhesion, especially desirable properties for optical applications.<sup>8</sup> Indeed, several optical applications—including second-harmonic generation<sup>9</sup> and light emission at 1.54  $\mu\text{m}$  in planar waveguides<sup>10</sup>—have been demonstrated in films grown by PLD.

In this letter we report the fabrication by alternating-target PLD of Cu nanocrystals embedded in an Al<sub>2</sub>O<sub>3</sub> matrix. The nanocomposite exhibits a large nonlinear index of refraction with significantly reduced saturable absorption compared to Cu:SiO<sub>2</sub> nanocomposites prepared by ion implantation. The Cu:Al<sub>2</sub>O<sub>3</sub> system was chosen since the linear and nonlinear optical properties of Cu nanocrystals produced by other techniques have been widely studied.<sup>11,12</sup> In addition, Al<sub>2</sub>O<sub>3</sub> has a high transparency and high refractive index, and optically doped Al<sub>2</sub>O<sub>3</sub> films with good properties have been previously grown by PLD.<sup>10</sup>

The films were deposited using an ArF excimer laser [193 nm, 12 ns full width at half maximum (FWHM), 5 Hz

repetition rate] focused alternately onto high-purity targets of Al<sub>2</sub>O<sub>3</sub> ceramic or metallic Cu, at a typical fluence of about 2 J cm<sup>-2</sup>. The targets were mounted in a computer-controlled holder 32 mm from the substrate, and rotated during ablation to prevent crater formation. The films were all grown in vacuum (10<sup>-7</sup> Torr) and the substrates were held at room temperature. The film thickness and deposition rate were monitored continuously by tracking the reflection coefficient of a He-Ne laser during PLD,<sup>13</sup> calibrated by *in situ* reflectivity curves from pure Al<sub>2</sub>O<sub>3</sub> and Cu films.

The nanostructure of the films was analyzed by high resolution (HR) transmission electron microscopy (TEM) of a sandwich structure of Al<sub>2</sub>O<sub>3</sub>/Cu/Al<sub>2</sub>O<sub>3</sub> deposited by PLD on carbon-coated mica substrates. The deposition sequence was 1500 pulses on the Al<sub>2</sub>O<sub>3</sub> target, then 160 pulses on the Cu target, followed by deposition of a top layer of Al<sub>2</sub>O<sub>3</sub> to prevent oxidation of the Cu nanoparticles. This configuration was chosen so that Cu nanocrystals from different layers did not overlap in the HRTEM images. HRTEM specimens were prepared by floating the films off the mica substrate in de-ionized water, then picking them up on a copper grid. They were analyzed in plan view using a JEOL 4000 EX transmission electron microscope operated at 400 kV (point-to-point resolution 0.16 nm). Figure 1(a) shows that the film exhibits a very homogeneous distribution of dark areas on a homogeneous background. In the HRTEM image [Fig. 1(b)], crystal lattice fringes from the Cu nanocrystals can be seen in the dark areas. The lack of order in the background contrast shows that the embedding Al<sub>2</sub>O<sub>3</sub> matrix is amorphous. From Fig. 1(b) we measured an average diameter of  $3 \pm 1 \text{ nm}$  for the Cu clusters, with an average crystallite separation of  $8 \pm 1 \text{ nm}$ , that is, twice the cluster diameter, which means that the nanoparticles are well isolated from each other. The density of crystallites in the film measured from the HRTEM images is  $2.1 \cdot 10^{12} \text{ cm}^{-2}$ . Figure 1 clearly shows that PLD in vacuum produces a more homogeneous spatial distribution of nanocrystallites with narrower size distribution than either sol-gel synthesis<sup>2</sup> or ion implantation.<sup>14</sup>

For optical characterization, Cu:Al<sub>2</sub>O<sub>3</sub> thin films were

<sup>a)</sup>Electronic mail: iodfv30@pinar1.csic.es

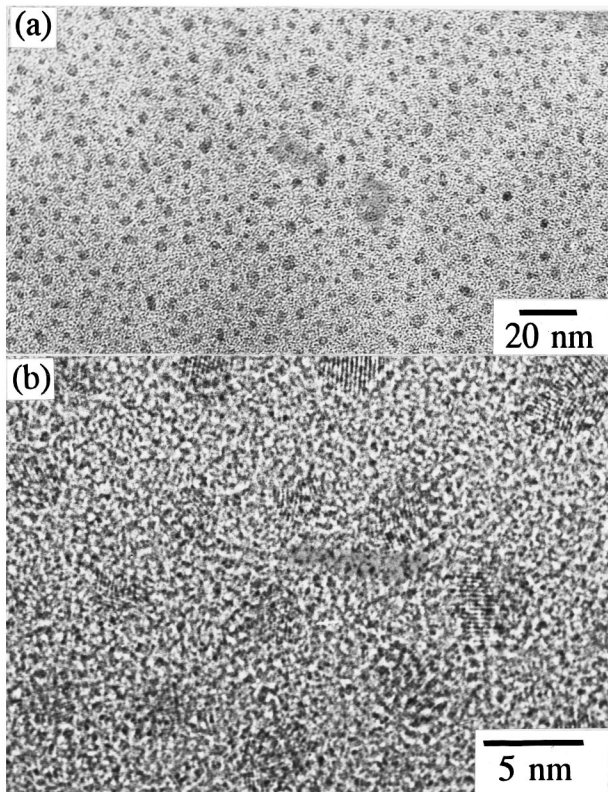


FIG. 1. TEM images of PLD  $\text{Al}_2\text{O}_3/\text{Cu}/\text{Al}_2\text{O}_3$  film. (b) is a HRTEM image, showing the presence of the interference fringes in the Cu clusters (dark areas).

grown under the same deposition conditions, but the  $\text{Al}_2\text{O}_3/\text{Cu}$  alternating structure was repeated up to 10 times, producing films  $190 \pm 10$  nm thick. The total Cu areal density was calculated from reflectivity curves to be  $1.3 \times 10^{17}$  atoms/cm<sup>2</sup>, comparable to Cu:SiO<sub>2</sub> nanocomposites produced by ion implantation.<sup>15</sup> The films were deposited on 0.1-mm-thick Corning glass substrates to minimize the substrate contribution to the optical measurements. An  $\text{Al}_2\text{O}_3$  reference sample with no Cu content was also grown.

Figure 2 shows that the absorption of the  $\text{Al}_2\text{O}_3$  reference film is negligible in the visible, showing its good optical quality. However, when Cu nanocrystals are present in the amorphous  $\text{Al}_2\text{O}_3$  matrix, the spectrum shows substantial absorption peaked around  $590 \pm 5$  nm, due to the surface plasmon resonance (SPR) of Cu nanoparticles.<sup>14</sup> The linear absorption coefficient of the film at the peak of the SPR is  $\alpha_0 = (40 \pm 4) \cdot 10^3 \text{ cm}^{-1}$ .

The nonlinear absorption coefficient ( $\beta$ ) and the nonlinear refractive index of the films were determined by  $z$ -scan.<sup>16</sup> The beam from a cavity-dumped, synchronously pumped, mode-locked dye laser tuned to 596 nm (pulse duration 6 ps, repetition rate 3.8 MHz) was focused by a 150 mm lens to a waist of 35  $\mu\text{m}$ , giving a maximum irradiance of  $4 \cdot 10^7 \text{ W cm}^{-2}$ . The Rayleigh range  $z_0$  of the beam was 6.2 mm, much longer than the thickness of either substrate or film. The on-axis transmission of the sample was measured by a small-aperture (SA) photodiode detector 90 cm from the lens; 8% of the total transmitted beam was split off just after the sample and monitored by an open-aperture (OA) detector. Both the SA and OA signals were normalized to incident

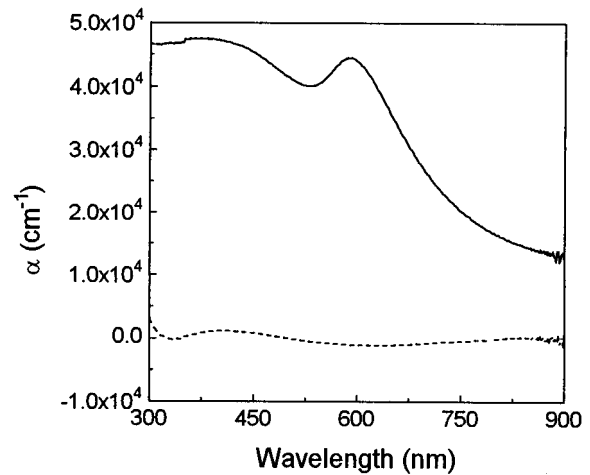


FIG. 2. Linear absorption coefficient ( $\alpha$ ) as a function of wavelength for the Cu: $\text{Al}_2\text{O}_3$ —and the  $\text{Al}_2\text{O}_3$  (--) film. Notice the appearance of the surface plasmon resonance peak at  $\approx 590$  nm when Cu nanoparticles are introduced in the  $\text{Al}_2\text{O}_3$  matrix.

laser power. The SA detector is sensitive both to nonlinear refraction and nonlinear absorption, the OA detector only to the latter. Each  $z$ -scan spectrum is a sequence of 700 points taken over the 40 mm interval in approximately 90 s; at each point, the photodiode signal is sampled 255 times, averaged and normalized to yield values for the OA and SA readings.

Figure 3 shows the variation of the OA and SA detector signals as a function of sample position ( $z$ ). The shape of the SA  $z$ -scan indicates a positive value for  $n_2$ , while the OA  $z$ -scan exhibits weak nonlinear saturation. The solid lines in Fig. 3 are the error-weighted, best chi-square fits to the data using a fitting function of the same form as Eq. (A4) of Ref. 16. The nonlinear phase shift incorporates both thermal and electronic contributions to the nonlinear refraction which are separable by their differing  $z$ -dependences:<sup>15</sup>

$$\Delta\Phi_{\text{el}} = \frac{kL \cdot n_2 I_0}{\left(1 + z^2/z_0^2\right)^2}, \quad (1a)$$

$$\Delta\Phi_{\text{th}} = kL \cdot \frac{dn}{dT} \Delta T = kL \cdot \frac{dn}{dT} \cdot \frac{P \alpha_0}{\kappa} \cdot \frac{1}{\left(1 + z^2/z_0^2\right)}. \quad (1b)$$

Here  $k$  is the wave number,  $L$  the sample thickness,  $T$  the temperature, and  $\kappa$  the thermal conductivity. The nonlinear saturation ( $\beta$ ), and the thermal ( $n_{2\text{th}}$ ) and electronic ( $n_{2e}$ ) components of the nonlinear refractive index ( $n_2$ ), were obtained from a global fit to OA and SA detector data from five different  $z$ -scan data scans taken at maximum intensities from  $2.1 \cdot 10^7$  to  $3.9 \cdot 10^7 \text{ W cm}^{-2}$ . The experimental values were  $\beta = -(2.34 \pm 0.18) \cdot 10^{-5} \text{ cm W}^{-1}$ ,  $n_{2e} = (2.93 \pm 1.08) \cdot 10^{-10} \text{ cm}^2 \text{ W}^{-1}$ , and  $n_{2\text{th}} = (1.24 \pm 0.18) \cdot 10^{-9} \text{ cm}^2 \text{ W}^{-1}$ .  $z$ -scans of the  $\text{Al}_2\text{O}_3$  reference film were flat, confirming that the Cu nanocrystals give rise to nonlinearity.

Near the SPR,  $n_{2e}$  is dominated by transitions from the  $d$  band to quantum-confined electrons in the  $s$ - $p$  conduction band.<sup>17</sup> Pump-probe<sup>12</sup> and four-wave mixing<sup>18</sup> experiments show that interband excitation of Cu:SiO<sub>2</sub> composites near the SPR is relaxed by fast electronic collisions within the nanocrystal on a scale of 1–4 ps, and by slower electron–

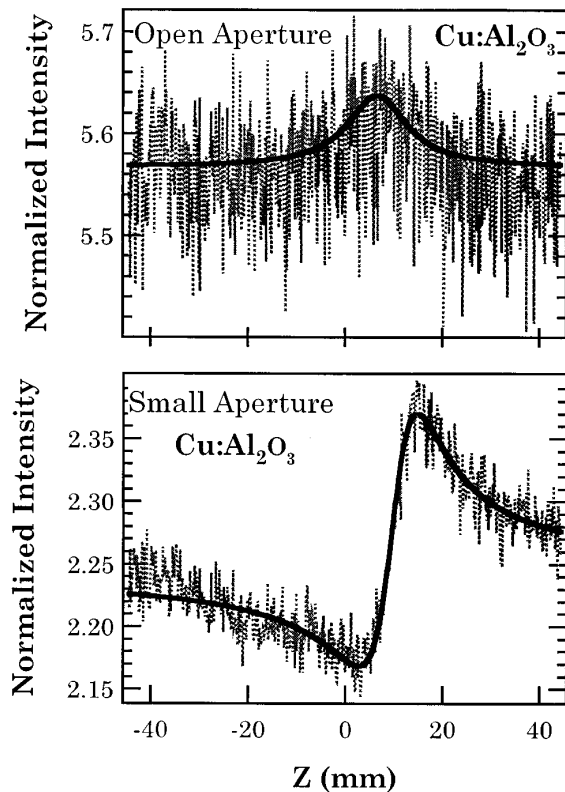


FIG. 3. Simultaneous open-aperture (OA) and small-aperture (SA)  $z$ -scans from the Cu:Al<sub>2</sub>O<sub>3</sub> film at a maximum intensity of  $3.7 \cdot 10^7$  W cm<sup>-2</sup>. The fainter dashed lines are the experimental data. The solid curves are the best-fit to the data.

phonon coupling to the matrix<sup>19</sup> ( $\sim 50$ – $200$  ps). Both processes are fluence- and size-dependent; in our experiment, relaxation times should be at the small end of the stated ranges. The real part of the electronic third-order susceptibility  $\chi^{(3)}$  is  $\text{Re}|\chi^{(3)}| \approx (2.06 \pm 0.77) \cdot 10^{-8}$  esu, within a factor of 2 of the value of  $|\chi^{(3)}|$  for Cu:SiO<sub>2</sub> off the SPR measured by a technique sensitive only to the electronic component of  $\chi^{(3)}$ .<sup>18</sup>

Compared to the nonlinear optical properties reported for Cu:SiO<sub>2</sub> samples made by ion implantation,<sup>14</sup> the nonlinear saturation in the PLD-grown material is two orders of magnitude smaller, whereas the nonlinear refractive index is of comparable magnitude; measurable nonlinear effects occur at an intensity almost an order of magnitude smaller. These differences may be attributed to the fact that PLD yields nanoparticles that are more homogeneous in diameter and in distribution than those obtained by other techniques, since both cluster distribution and shape influence the linear and nonlinear optical properties of the nanocomposite.<sup>20</sup>

In summary, we have demonstrated that PLD in vacuum produces composites in which Cu nanocrystals with a remarkably homogeneous spatial and size distributions are embedded in Al<sub>2</sub>O<sub>3</sub>. The nonlinear refractive index for the Cu:Al<sub>2</sub>O<sub>3</sub> films made by PLD is as large as that obtained for films made by other techniques, while the nonlinear saturation parameter is two orders of magnitude lower. The results thus show the excellent potential of PLD for producing nanocrystal-composite thin films in a single-step fabrication process, requiring no post-deposition treatments to optimize the optical or structural properties of the samples.

The authors are indebted to Dr. R. H. Magruder, III for the use of a dual-beam spectrophotometer. This project was partially supported by CICYT (Spain) under Contract No. TIC96-0467 and by the U.S. Army Research Office Grant No. (DAAH04-93-G-0123).

- <sup>1</sup>K. Lu, T. Wang, and W. D. Wei, *J. Appl. Phys.* **69**, 522 (1991).
- <sup>2</sup>G. De, L. Tapfer, M. Catalano, G. Battaglin, F. Caccavale, F. Gonella, P. Mazzoldi, and R. F. Haglund, Jr., *Appl. Phys. Lett.* **68**, 3820 (1996).
- <sup>3</sup>H. B. Liao, R. F. Xiao, J. S. Fu, P. Yu, G. K. L. Wong, and Ping Sheng, *Appl. Phys. Lett.* **70**, 1 (1997).
- <sup>4</sup>P. Mazzoldi, G. W. Arnold, G. Battaglin, R. Bertocello, and F. Gonella, *Nucl. Instrum. Methods Phys. Res. B* **91**, 478 (1994).
- <sup>5</sup>R. A. Wood, P. D. Townsend, N. D. Skelland, D. E. Hole, J. Barton, and C. N. Afonso, *J. Appl. Phys.* **74**, 5754 (1993).
- <sup>6</sup>K. Fukumi, A. Chayahara, K. Kadono, T. Sakaguchi, Y. Horino, M. Miya, K. Fujii, J. Hayakawa, and M. Satou, *J. Appl. Phys.* **75**, 3075 (1994).
- <sup>7</sup>S. Ohtsuka, T. Koyama, K. Tsunetomo, H. Nagata, and S. Tanaka, *Appl. Phys. Lett.* **61**, 2953 (1992).
- <sup>8</sup>C. N. Afonso, in *Insulating Materials for Optoelectronics*, edited by F. Agulló-López (World Scientific, Singapore, 1995), Ch. 1, p. 1.
- <sup>9</sup>Fulin Xiong, R. P. H. Chang, M. E. Hagerman, V. L. Kozhevnikov, K. R. Poepelmeier, H. Zhou, G. K. Wong, J. B. Ketterson, and C. W. White, *Appl. Phys. Lett.* **64**, 161 (1994).
- <sup>10</sup>R. Serna and C. N. Afonso, *Appl. Phys. Lett.* **69**, 1541 (1996).
- <sup>11</sup>K. Uchida, S. Kaneko, S. Omi, C. Hata, H. Tanji, Y. Asahara, A. J. Ikushima, T. Tokizaki, and A. Nakamura, *J. Opt. Soc. Am. B* **11**, 1236 (1994).
- <sup>12</sup>J.-Y. Bigot, J.-C. Merle, O. Cregut, and A. Daunois, *Phys. Rev. Lett.* **75**, 4702 (1995).
- <sup>13</sup>C. N. Afonso, F. Vega, J. Gonzalo, and C. Zaldo, *Appl. Surf. Sci.* **69**, 149 (1993).
- <sup>14</sup>R. H. Magruder, III, Li Yang, R. F. Haglund, Jr., J. E. Wittig, and R. A. Zuhr, *J. Appl. Phys.* **76**, 708 (1994).
- <sup>15</sup>R. F. Haglund, Jr., Li Yang, R. H. Magruder III, J. E. Wittig, K. Becker, and R. A. Zuhr, *Opt. Lett.* **18**, 373 (1993).
- <sup>16</sup>M. Sheik-Bahae, A. A. Said, T. Wei, D. J. Hagan, and E. W. Van Stryland, *IEEE J. Quantum Electron.* **26**, 760 (1990).
- <sup>17</sup>C. Flytzanis, F. Hache, M. C. Klein, D. Ricard, and Ph. Roussignol, "Nonlinear optics in composite materials," edited by E. Wolf, in *Progress in Optics XXIX* (Elsevier Science, Amsterdam, 1991), Ch. 5.
- <sup>18</sup>Li Yang, K. Becker, F. M. Smith, R. H. Magruder III, R. F. Haglund, Jr., Lina Yang, R. Dorsinville, R. R. Alfano, and R. A. Zuhr, *J. Opt. Soc. Am. B* **11**, 457 (1994).
- <sup>19</sup>T. Tokizaki, A. Nakamura, S. Kaneko, K. Uchida, S. Omi, H. Tanji, and Y. Asahara, *Appl. Phys. Lett.* **65**, 941 (1994).
- <sup>20</sup>U. Kreibig and M. Vollmer, in *Optical Properties of Metal Clusters* (Springer, Berlin, 1995), pp. 53–63.